

## CHARACTERIZATION AND ANALYSIS OF InGaN PHOTOVOLTAIC DEVICES

Omkar Jani<sup>1</sup>, Christiana Honsberg<sup>2</sup>, Ali Asghar<sup>1</sup>, David Nicol<sup>1</sup>, Ian Ferguson<sup>1</sup>, Alan Doolittle<sup>1</sup>, Sarah Kurtz<sup>3</sup>

1. School of Electrical and Computer Engineering, Georgia Institute of Technology, Atlanta, GA 30332
2. School of Electrical and Computer Engineering, University of Delaware, Newark, DE 19716
3. National Renewable Energy Laboratories, Golden, CO 80401

### ABSTRACT

The InGaN material system is investigated to achieve high efficiency solar cells, using tandem and quantum-well structures to implement high efficiency concepts. Here InGaN p-i-n and quantum-well solar cells are designed, grown by MOCVD and fabricated into mesa devices. They are electrically characterized by I-V response under dark, white light and UV illumination and internal quantum efficiency (IQE). Material characterization is done by X-ray diffraction, photoluminescence and photoemission. InGaN solar cells with high In compositions are grown in two configurations, one incorporating it into the i-region of a p-i-n solar cells, and the other incorporating as the well-region of a quantum-well device. A QE of 8% was measured from these quantum-wells. Solar cells with In lean In<sub>0.07</sub>Ga<sub>0.93</sub>N p-i-n device structures show an IQE of 19% as well as photoemission at 500nm, confirming the suitability of the material for photovoltaic applications.

### INTRODUCTION

The InGaN material system offers a substantial potential to develop ultra-high efficiency solar cells. With the remeasurement of the bandgap of In at ~0.7eV [1,2,3] the bandgap of the InGaN material system ranges the major bulk of the solar spectrum including the visible region. A continuum of bandgaps can be obtained by changing the compositions of In and Ga making it relatively easier for MBE and MOCVD growth processes limiting the number of material sources. InGaN also has an apparent insensitivity to high dislocation densities as the polarization and piezoelectric properties of the material introduce electric fields and surface dipoles that may counter the effect of dislocations. Additional advantages include low effective mass of electrons and holes, high mobilities, high peak and saturation velocities [4], high absorption coefficients and radiation tolerance.

The In-lean, high band gap end of the material system, typically grown by MOCVD, is extensively used for LEDs [5]. While the band gap of blue LEDs at 3.4 eV is higher than the optimal range for a solar cell, the more recently emerging green LEDs are useful for high band gap devices in tandems with 5 junctions or greater. High In content, low band gap material grown by MBE, due to its more recent identification as a potential device material, is less well understood and is presently less used in

devices. It is the subject of major fundamental material characterization.

For both kinds of materials, there are several critical issues in determining their potential and use in photovoltaic applications, primarily relating to the collection efficiency and recombination rates, which in turn depend critically on the minority carrier lifetime. Modeling indicates that the radiative lifetimes of InN alloys should be similar or higher than those of GaN [6]. However, experimental lifetimes of minority carriers in these materials are currently dominated by the material quality as it is a newly emerging material system.

Achieving p-type conductivity in InGaN alloys is difficult partly due to a high background concentration of electrons. P-type GaN can be achieved by improving the structural quality of GaN, but still has a limit of less than  $10^{18}\text{cm}^{-3}$  hole concentration due to the deep activation energy of acceptors [7]. Practical InGaN has been shown to possess higher background electron concentrations of about  $10^{19}\text{cm}^{-3}$  which compensates the holes [8]. No report of p-type conductivity over the entire region thickness has yet been given for In composition greater than 32% indicating that p-type InGaN may be a challenge to obtain.

A unique feature for the III-nitrides is strong polarization and piezoelectric effects [9,10]. These are highly polar molecules, and hence, develop a large dipole at interfaces between the materials inducing an electric field in the bulk region between two surfaces. Piezoelectric fields may also be induced in the material by strain from lattice mismatch. The high piezoelectric coefficients modify the surface potentials and generate electric fields across the materials, and hence are critical in the interpretation of transport properties of the material [11].

Sapphire is the most common substrate for growth of wurtzite GaN. However, due to the large lattice and thermal mismatches between sapphire and GaN of 16%, epitaxial films on sapphire result in dislocation densities typically in the  $10^7$  to  $10^{10}\text{cm}^{-2}$  range.

### THEORY

Tandem cells are constructed by stacking solar cells with decreasing bandgaps with the greatest bandgap on top. The top cells efficiently absorb the high energy photons minimizing thermalization losses and allowing

lower energy photons to transmit through it. Maximum theoretical efficiency obtained by such selective absorption from an infinite stack of tandem cells is 86.8%. Detailed balance modeling was performed for tandem devices with 4 to 8 bandgaps using a concentration of 500x and a spectrum of 6000K to calculate the optimum bandgaps [12] and are summarized in table 1.

Table 1. Values of Bandgaps and Efficiencies of 4 to 8 Stack Tandem Cells at Concentration of 500x and Spectrum of 6000K.

n	Values of Band Gap (eV)	$\eta$ %
4	0.60, 1.11, 1.69, 2.48	62.0
5	0.53, 0.95, 1.40, 1.93, 2.68	65.0
6	0.47, 0.84, 1.24, 1.66, 2.18, 2.93	67.3
7	0.47, 0.82, 1.19, 1.56, 2.0, 2.5, 3.21	68.9
8	0.44, 0.78, 1.09, 1.4, 1.74, 2.14, 2.65, 3.35	70.2

The bandgaps of interest in this paper are the high bandgaps greater than 2eV and the low bandgap materials which are less than 1eV. MOCVD is an established technology to grow the high bandgap materials, while MBE is the technology of choice for the extremely low bandgap materials.

Two types of structures are primarily investigated here: p-i-n and quantum-well solar cells. P-i-n structures may have the i-region of a same or different bandgap. The thickness of the i-region is maximized to extend the region with electric field for efficient absorption and collection of photogenerated carriers. The p and n junctions used are GaN due to its established quality from optimized MOCVD growth. Moreover, they are used as window layers in order to maximize the absorption of the targeted wavelengths in the i-layer for maximum collection and thus, characterization.

Quantum-wells are very thin layers of bandgap lower than that of the junction and i-regions. Here they are incorporated in the i-region where an electric field is maintained across it. They appear as wells in the energy band diagram of the device, and hence the term - wells. These low dimension structures exhibit energy levels within the wells which maintain carriers for a particular lifetime after which they escape or recombine. Hence, the quantum-well behaves as a superposition of materials with bandgaps corresponding to the differences in energy levels of various bands. The various mechanisms for escape of carriers are subsequent absorption of light, thermal escape using ambient thermal energy and tunneling.

The quantum-wells used in present experiments are not used to provide theoretical increases in efficiency via the multiple absorption processes introduced by the different energy levels, but rather to achieve high quality layers with higher In composition into high band gap solar cells. Here, thin layers (in orders of Angstroms) of InGaN are grown on GaN at regular intervals to obtain high quality InGaN. The quantum-well devices fabricated in this manner are used to characterize low bandgap InGaN.

## DESIGN

InGaN with bandgap over 2V grown by MOCVD is tested as a photovoltaic material in this paper. Hence,  $\text{In}_{0.4}\text{Ga}_{0.6}\text{N}$  p-i-n and quantum-well solar cells were designed as the first set of devices. The bandgap of  $\text{In}_{0.4}\text{Ga}_{0.6}\text{N}$  is calculated to be about 2eV using a bowing factor of 1.4eV [13]. The main goal of the device design is to maximize absorption and collection from the InGaN material under study. As this material is used as the i-region of the p-i-n structure and it is intended to maximize the thickness of this field bearing region, the thickness of the p and n junctions need to be minimal. The electric field is maximized by doping the p and n junctions as high as possible consistent with good material quality. There is a tradeoff as increasing the i-region thickness decreases the electric field in it. Moreover, due to background n doping present in as-grown intrinsic material, a uniform electric field cannot be maintained throughout the i-region. Thus, the electric field limits the i-region thickness at the cost of absorption. From energy band simulations by PC1D, it was found that a strong electric field extends only up to a depth of 200nm from the p-region into the i-region after which it rapidly decreases to zero. Hence, the i-region thickness has to be limited to 200nm to maintain drift transport of charges across it. The MOCVD growth process was optimized for a maximum doping of  $2 \times 10^{17} \text{cm}^{-3}$  for Mg (p-type) and  $4 \times 10^{18} \text{cm}^{-3}$  for Si (n-type) for GaN. Hence, an average theoretical electric field of 0.31kV/cm was obtained across the i-region.

Measured minority lifetimes upto 6.5ns for GaN have been reported [14,15], while electron and hole mobilities of  $1000 \text{cm}^2/\text{V-s}$  and  $200 \text{cm}^2/\text{V-s}$  have been calculated [16]. However, electron and hole respective mobilities of  $400 \text{cm}^2/\text{V-s}$  and  $10 \text{cm}^2/\text{V-s}$  had been achieved previously grown samples in the lab and a recombination lifetime of 2ns was assumed. The calculated electron and hole diffusion lengths from these values were  $1.44 \mu\text{m}$  and  $0.2 \mu\text{m}$  respectively. The value of the hole diffusion length limits the thickness of the n-layer to 200nm, while there is enough leeway in the maximum thickness of the p-region. The p-region was intended to be as thin as possible, but at the same time be able to provide charge for the junction and the top metal contact. Hence, a p-layer thickness value of 80nm to 100nm was accepted from modeling of energy bands in PC1D.

The quantum-well device was designed as a GaN p-i-n cell with five 1nm  $\text{In}_{0.4}\text{Ga}_{0.6}\text{N}$  layers in the i-region spaced at about 14nm to prevent any mutual coupling effects. The difference between the first hole and electron energy levels in the 1nm thick  $\text{In}_{0.4}\text{Ga}_{0.6}\text{N}$  quantum-well is about 2.68eV that corresponds to a wavelength of 460nm. The calculated absorption coefficient for the well at this energy was  $115390 \text{cm}^{-1}$ . For this value, 5 wells of 1nm thickness absorb a total of 56% of the incident light entering through the GaN window layers, and hence were expected to give a substantial photo-response. This quantum-well structure is shown in figure 1.

A second set of p-i-n cells were fabricated incorporating high bandgap  $\text{In}_{0.07}\text{Ga}_{0.93}\text{N}$  in the i-region. The calculated bandgap of  $\text{In}_{0.07}\text{Ga}_{0.93}\text{N}$  is 3.1eV, which is

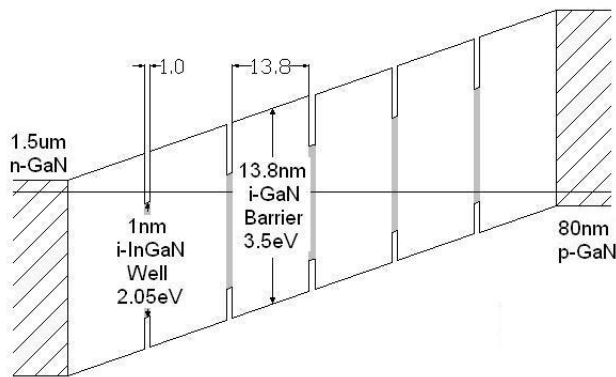


Fig. 1. Band Diagram of Quantum-Well Solar Cell.

close to the top cell bandgaps in tandem cells with a large number of junctions. It is possible to obtain good quality  $\text{In}_{0.07}\text{Ga}_{0.93}\text{N}$  from MOCVD as its structure and growth conditions are close to that of GaN, and hence, successfully characterize it as a photovoltaic material.

One major constraint on the n-layer thickness is introduced due to fabrication issues. Individual devices are isolated into mesas during fabrication by Inductively Coupled Plasma (ICP) etching up to the middle of the n-layer as shown in figure 2. Hence, the thickness of the n-layer should be greater than the tolerance level of the ICP etch process.

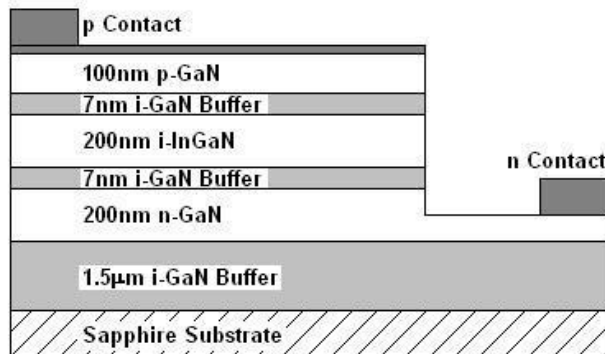


Fig. 2. P-i-n Solar Cell Structure.

Structures figure 2 and described previously were thus designed from preliminary calculations. The overall thickness of the cell was designed to be 500 nm which absorbs 95% of the targeted incident light. The major challenges for fabrication of these cells were to incorporate reasonably thick layers of crystalline InGaN with a high In content by MOCVD growth.

## EXPERIMENT

Two p-i-n and one quantum-well solar cell structures were grown by MOCVD. The quantum-well solar cell consisted of GaN junction and barrier materials with five  $\text{In}_{0.4}\text{Ga}_{0.6}\text{N}$  quantum-wells of 1 nm thickness in the i-region shown in figure 1. The GaN barriers were 13.8 nm thick. The top p-layer thickness was 80 nm doped at  $2 \times 10^{17} \text{ cm}^{-3}$ , while the bottom n-layer was 1.5 μm thick doped at  $4 \times 10^{18} \text{ cm}^{-3}$  as it also worked as a buffer layer for the i-layer

during growth. The GaN buffer layer minimizes the dislocations propagating from the lattice mismatch of the sapphire substrate and GaN into the i-region of the device.

Both the p-i-n devices consisted of 100 nm thick  $2 \times 10^{17} \text{ cm}^{-3}$  p-GaN and 200 nm thick  $4 \times 10^{18} \text{ cm}^{-3}$  n-GaN. The first p-i-n cell consisted of  $\text{In}_{0.4}\text{Ga}_{0.6}\text{N}$  in the i-region. A 1.5 μm thick undoped GaN layer was used as a buffer to grow 200 nm n-GaN. An undoped GaN layer of 7 nm thickness was grown as a buffer to recover the quality of substrate for growth of InGaN. For the  $\text{In}_{0.4}\text{Ga}_{0.6}\text{N}$  p-i-n device, the thickness of i-region was limited to 130 nm during growth due to possibility of material degradation at a higher thickness. Another similar 7 nm thick i-GaN buffer layer was used before growing the top p-GaN layer.

The second p-i-n cell was fabricated with an i-layer of  $\text{In}_{0.07}\text{Ga}_{0.93}\text{N}$ .  $\text{In}_{0.07}\text{Ga}_{0.93}\text{N}$  has a bandgap of 3.1 eV and was used to ensure fabrication of a high quality test p-i-n structure to study the behavior of such devices. A top view of completely fabricated structure of this p-i-n cell is shown in figure 3, with the lit area corresponding to light emission from a single device under forward bias.

The material was fabricated into mesa devices by Inductively Coupled Plasma (ICP) Etch. The top of the cell was coated with a thin Ni-Au transparent contact. A 50 nm thick p-bonding pad was deposited for external contact. The n-contact consists of 50 nm thick Ti-Al-Ti-Au layer. The area of each individual device was  $320 \mu\text{m} \times 320 \mu\text{m}$  as shown in the figure.

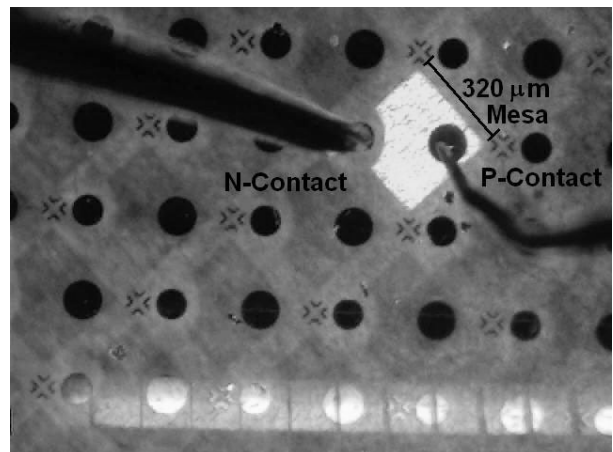


Fig. 3. Fabricated  $\text{In}_{0.07}\text{Ga}_{0.93}\text{N}$  p-i-n solar cell mesa structure emitting light at 500 nm wavelength at a supply voltage of about 3V.

## RESULTS

Photoluminescence and x-ray diffraction measurements were performed to characterize the material while I-V and Internal Quantum Efficiency (IQE) measurements were done for electrical characterization of the device.

The I-V measurements were taken under dark conditions, white light as well as in presence of a UV light source. The I-V curve of the quantum-well sample is shown in figure 4. Photo-response of the device to white as well as UV light is seen from the figure. The left shift of the curve under illumination shows an opposing effect of a

second diode in series which may be due to the GaN – metal contact interface. The downward shift of the curve under UV illumination shows a significant additional response to UV light.

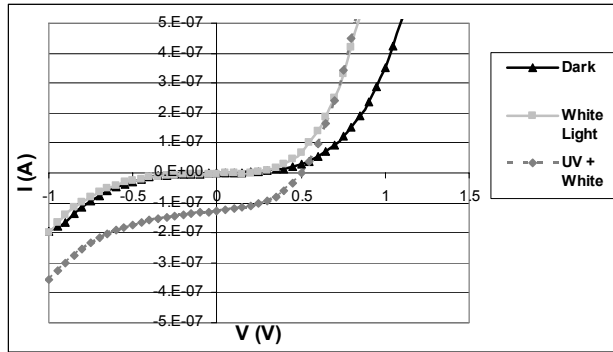


Fig. 4. I-V Curve for Quantum-Well Device under various illuminations.

The photoluminescence data from the material used for the QW device at different parts of the sapphire wafer is shown in figure 5.

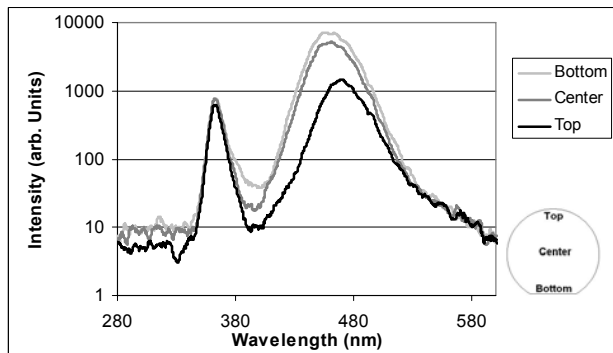


Fig. 5. Photoluminescence for Quantum-Well Device at top, center and bottom of the substrate.

Strong photoluminescence peaks are observed at 365nm from GaN and a relatively stronger and broader one at 460nm for the InGaN quantum-wells. Slightly poorer quality growth is observed at the top sites of the wafer as they are situated away from the center of the chamber during the MOCVD growth process.

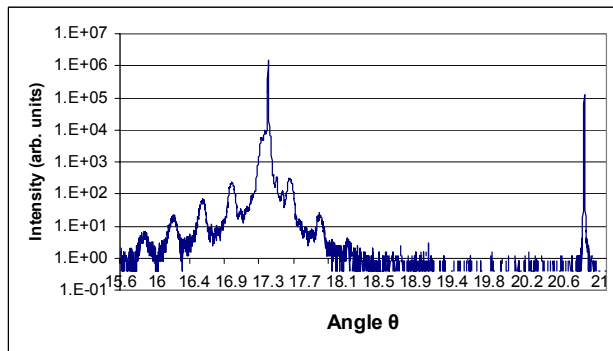


Fig. 6. X-Ray data for Quantum-Well Device.

The quantum-well structures are clearly seen in the X-ray diffraction data in figure 6. The GaN peak is seen at  $\theta=17.28^\circ$ , while subsequent peaks correspond to the InGaN quantum-well material with 40% In composition and their lower order harmonics. From further analysis, the thickness of the quantum-wells and barriers were confirmed at 1nm and 13.8nm respectively. Moreover, the distinct peaks verify the growth of a good quality crystalline heterostructure.

The I-V curve of the  $\text{In}_{0.4}\text{Ga}_{0.6}\text{N}$  p-i-n sample is shown in figure 7. It is seen that the cell hardly responds to white light, while gives a significant response to UV illumination. Again, an opposing diode effect is seen here similar to the quantum-well device most probably due to the Schottky barrier at the GaN-Metal contact interface.

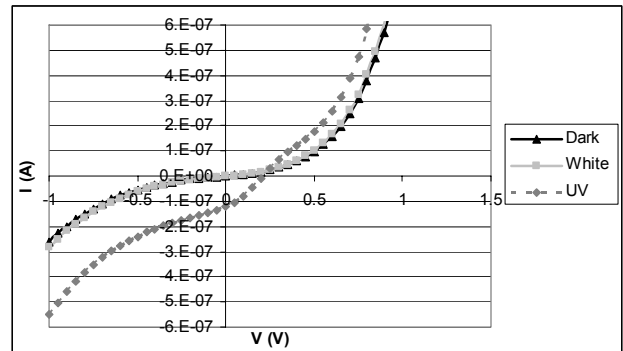


Fig. 7. I-V Curve for p-i-n cell with  $\text{In}_{0.4}\text{Ga}_{0.6}\text{N}$  as the i-layer.

Figure 8 shows the x-ray diffraction data for the  $\text{In}_{0.4}\text{Ga}_{0.6}\text{N}$  cell. The poor crystalline quality of the material is evident from the graph and reveals a completely relaxed nature of the  $\text{In}_{0.4}\text{Ga}_{0.6}\text{N}$  layer. However, the In composition in the material is confirmed at 40%. A poor photoluminescence is also observed for this structure implying a heavily defected material.

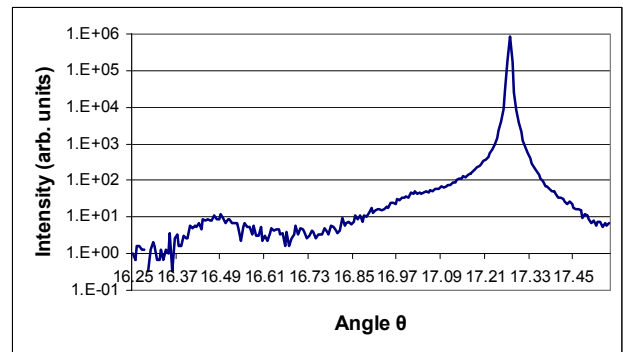


Fig. 8. X-ray -V data for p-i-n cell with  $\text{In}_{0.4}\text{Ga}_{0.6}\text{N}$  as the i-layer.

The I-V curve of the  $\text{In}_{0.07}\text{Ga}_{0.93}\text{N}$  device is shown in figure 9. The bandgap corresponding to InGaN with an In composition of 7% is about 3.1eV. This high bandgap is supported by the marginal response to white light as seen from the I-V curve. The device shows a substantial photo-response UV illumination giving a distinct  $V_{oc}$  of 2V.

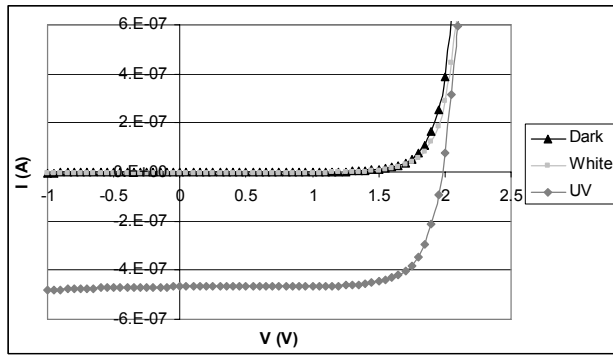


Fig. 9. I -V Curve for p-i-n cell with  $\text{In}_{0.07}\text{Ga}_{0.93}\text{N}$  as the i-layer.

Emission of green light at 500nm wavelength was observed during the I-V sweep of the device as shown in figure 10. This 500nm corresponds to a bandgap of 2.48 implying the presence of a high quality low bandgap InGaN material with In composition of 27%.

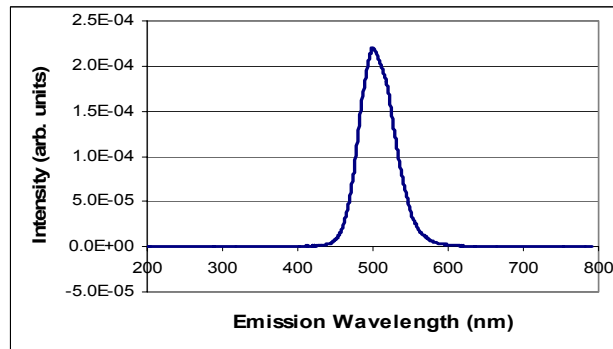


Fig. 10. Emission Spectra of  $\text{In}_{0.07}\text{Ga}_{0.93}\text{N}$  p-i-n cell.

The photoluminescence data for this device is shown in figure 11. Two PL peaks, a broad peak at 510nm, and a narrower but stronger peak at 500nm, are observed in the spectra. This corresponds to InGaN material with In composition of 27% corresponding to the 500nm emission and that of 28% corresponding to the 510nm emission. No photoluminescence is seen at 400nm wavelength which corresponds to the targeted In composition of 7%.

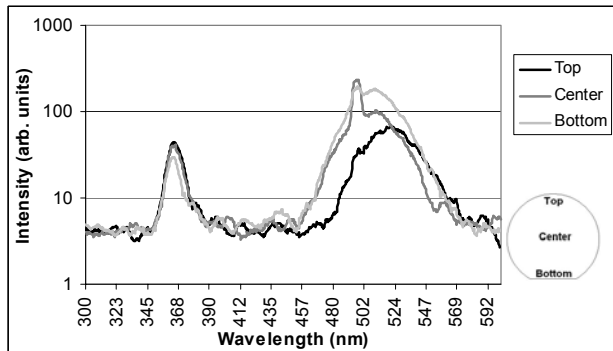


Fig. 11. Photoluminescence Spectra for  $\text{In}_{0.07}\text{Ga}_{0.93}\text{N}$  p-i-n device.

The X-ray data in figure 12 shows a broad range of In composition in the InGaN i-region. This In composition ranges from 3% to 16% with the maximum intensity at 7%. This peak corresponds to the targeted bandgap of 3.1 eV for the material. A strong peak at  $\theta=17.28^\circ$  is observed representing good quality GaN.

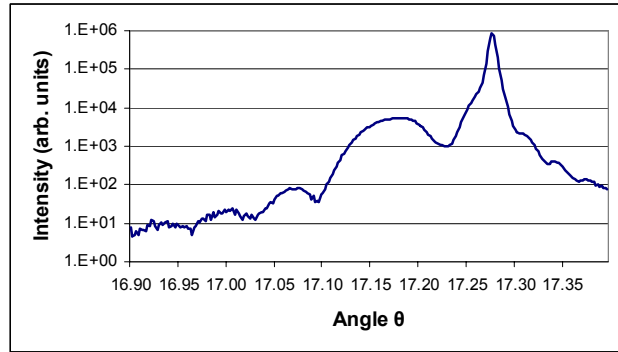


Fig. 12. X-ray -V data for p-i-n cell with  $\text{In}_{0.07}\text{Ga}_{0.93}\text{N}$  as the i-layer.

Figure 13 shows the IQE data for all the three devices. It can be seen that the  $\text{In}_{0.4}\text{Ga}_{0.6}\text{N}$  p-i-n cell has a very weak photo-response due to its poor material quality. This fact is supported by a weak photoluminescence signal and x-ray data. The quantum-well device gives a reflection-corrected QE of 8% at 350nm gradually decreasing till about 470nm under bias light. This bandgap of the semiconductor determined from IQE data is 2.7eV which corresponds to the transition between the first electron and hole energy levels of the  $\text{In}_{0.4}\text{Ga}_{0.6}\text{N}$  quantum-well. The low efficiency is primarily due to incomplete absorption of light by the thin wells. An IQE of 19% is observed for the  $\text{In}_{0.07}\text{Ga}_{0.93}\text{N}$  p-i-n device. A distinct drop in IQE is seen at 400nm confirming the bandgap of the material at 3.1eV.

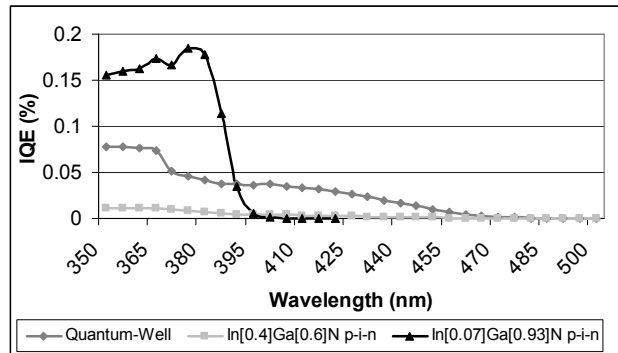


Fig. 13. Internal Quantum Efficiency for (i) Quantum-well, (ii)  $\text{In}_{0.4}\text{Ga}_{0.6}\text{N}$  and (iii)  $\text{In}_{0.07}\text{Ga}_{0.93}\text{N}$  p-i-n device. Note: Discontinuity at 370nm is due to change in slit width during measurement.

## DISCUSSION

Comparing the results of  $\text{In}_{0.4}\text{Ga}_{0.6}\text{N}$  p-i-n and quantum-well structures, the quality in the quantum-well is

far more superior as a photovoltaic material than that in the p-i-n structure. This fact is supported by the strong photoluminescence in agreement to the theoretical value of 460nm, a QE of 8% in spite of transmission losses and x-ray diffraction data. Hence, low bandgap InGaN can be incorporated in devices in the form of heterostructures. Moreover, from the response to white light, it can be inferred that the quantum-well effective bandgaps can be used to absorb light of very low energy used as bottom cells of ultra-high efficiency tandems.

An opposing current was observed from the I-V curve of the two devices under white light and UV illumination. This is most probably caused by a light activated Schottky contact at the p-GaN - metal interface requiring further investigation.

A high quality p-i-n solar cell was fabricated using the high bandgap  $\text{In}_{0.07}\text{Ga}_{0.93}\text{N}$ . This fact is supported by the distinct I-V curves and an IQE of 19%. Hence, this high quality crystalline material is an excellent candidate for high performance solar cells.

However, the In-composition in the material is not consistent throughout the structure. This is evident from the x-ray diffraction and photoluminescence and supported by the I-V curves. The x-ray shows a range of In composition in the bulk InGaN centered around the targeted 7%. The IQE also confirms the bandgap of 3.1eV. But the photoluminescence and photoemission peaks show a high quality phase separated InGaN consisting of 27% In. Moreover, this thin layer acts as the recombination site and is responsible for emission of green light from the sample. This phase separated material is consistent with the low Voc of the solar cell at 2V instead of the expected Voc at about 2.6V.

## CONCLUSION

InGaN with bandgap over 2V grown by MOCVD is tested as a photovoltaic material. Two kinds of devices with two distinct InGaN materials were designed, grown, fabricated and characterized.  $\text{In}_{0.4}\text{Ga}_{0.6}\text{N}$  incorporated in quantum-wells showed superior performance with a QE of 8% compared to the p-i-n device. Hence, quantum-wells can be used to incorporate materials that are hard to grow as thicker layers. A successful high bandgap InGaN p-i-n solar cell was fabricated giving an IQE of 19%. The phase separated lower bandgap InGaN dominated and dropped the Voc to about 2V instead of the expected 2.6V signifying the importance of In uniformity in the material. These results suggest InGaN as an excellent candidate for high efficiency photovoltaic applications and practical methods to implement them.

## ACKNOWLEDGEMENTS

This work was partially supported by U.S. D.O.E. and the National Renewable Energy Laboratories, monitored by Dr. Robert McConnell and Dr. Martha Symko-Davies and the Office of Naval Research, monitored by Dr. Colin Wood.

## REFERENCES

- [1] V. Yu. Davydov et al., "Absorption and Emission of Hexagonal InN. Evidence of Narrow Fundamental Band Gap", *Phys. Stat. Sol. B*, **229**, 3, 2002, pp. R1-R3.
- [2] J. Wu et al., "Temperature Dependence of the Fundamental Band Gap of InN", *J. Appl. Phys.*, **94**, 7, 2003, pp. 4457-4460.
- [3] T. Matsuoka, H. Okamoto, M. Nakao, H. Harima, and E. Kurimoto, "Optical Bandgap Energy of Wurtzite InN", *Appl. Phys. Lett.*, **81**, 7, 2002, pp. 1246-8.
- [4] Y. Nanishi, Y. Saito and T. Yamaguchi, "R-F Molecular Beam Epitaxy Growth and Properties of InN and Related Alloys", *Jpn. J. Appl. Phys.*, **42**, 5A, 2003, pp. 2549-2559.
- [5] S. Nakamura, S. Pearton and G. Fasol, "The blue laser diode, 2 ed", Springer-Verlag, 2000.
- [6] A. Dmitriev and A. Oruzhenikov, "The rate of radiative recombination in nitride semiconductors and alloys," *J. Appl. Phys.*, **86**, 6, 1999, 3241-3246.
- [7] T. Tanaka et al., "P-type Conduction in Mg-doped GaN and  $\text{Al}_{0.08}\text{Ga}_{0.92}\text{N}$  Grown by Metalorganic Vapor Phase Epitaxy", *Appl. Phys. Lett.*, **65**, 5, 1994, pp. 593-594.
- [8] W. Geerts, J.D. Mackenzie, C.R. Abernathy, S.J. Pearton, and T. Schmiedel, "Electrical transport in p-GaN, n-InN and n-InGaN", *Solid-State Electron.*, **39**, 9, 1996, pp. 1289-1294.
- [9] F. Bernardini, and V. Fiorentini, "Nonlinear Macroscopic Polarization in III-V Nitride Alloys", *Phys. Rev. B*, **64**, 8, 2001, pp. 085207/1-7.
- [10] V. Fiorentini F. Bernardini, "Spontaneous versus Piezoelectric Polarization in III-V Nitrides: Conceptual Aspects and Practical Consequences", *Phys. Stat. Sol. B*, **216**, 1, 1999, pp. 391-398.
- [11] O. Ambacher et al., "Two-dimensional electron gases induced by spontaneous and piezoelectric polarization charges in N- and Ga-face AlGaIn/GaN heterostructures", *J. Appl. Phys.*, **85**, 6, 1999, pp. 3222-3233.
- [12] A. Devos, "Endoreversible Thermodynamics of Solar Energy Conversion", Oxford Univ. Pr., 1992.
- [13] J. Wu et al., "Small Bandgap Bowing in  $\text{In}_x\text{Ga}_{1-x}\text{N}$  Alloys", *Appl. Phys. Lett.*, **80**, 25, 2002, pp. 4741-4743.
- [14] Z.Z. Bandic, P.M. Bridger, E.C. Piquette and T.C. McGill, "Minority carrier diffusion length and lifetime in GaN", *Appl. Phys. Lett.*, **72**, 24, 1998, pp. 3166-3168.
- [15] Y. Narukawa, S. Saijou, Y. Kawakami, S. Fujita, T. Mukai, and S. Nakamura, "Radiative and Nonradiative Recombination Processes in Ultraviolet Light-Emitting Diode Composed of an  $\text{In}_{0.02}\text{Ga}_{0.98}\text{N}$  Active Layer", *Appl. Phys. Lett.*, **74**, 4, 1999, pp. 558-560.
- [16] M.E. Levinshtein, S.L. Rumyantsev and M.S. Shur, "Properties of Advanced Semiconductor Materials: GaN, AlN, InN, BN, SiC, SiGe", John Wiley & Sons, Inc., New York, 2001.